

Canceling spin-dependent contributions and systematic shifts in precision spectroscopy of molecular hydrogen ions

S. Schiller*

Institut für Experimentalphysik, Heinrich-Heine-Universität Düsseldorf, 40225 Düsseldorf, Germany

V. I. Korobov

Bogoliubov Laboratory of Theoretical Physics, Joint Institute for Nuclear Research, 141980 Dubna, Russia

(Received 8 May 2018; published 15 August 2018)

We consider the application of a basic principle of quantum theory, the tracelessness of a certain class of Hamiltonians, to the precision spectroscopy of the molecular hydrogen ions. We show that it is possible to obtain the spin-averaged transition frequencies between states from a simple weighted sum of experimentally accessible spin-dependent transition frequencies. We discuss the cases H_2^+ and HD^+ , which are distinct in the multipole character of their rovibrational transitions. Inclusion of additional frequencies permits canceling also the electric quadrupole shift, the Zeeman shift, and partially the Stark shift. In this context, we find that measuring electric quadrupole transitions in the heteronuclear molecule HD^+ is advantageous. The required experimental effort appears reasonable.

DOI: [10.1103/PhysRevA.98.022511](https://doi.org/10.1103/PhysRevA.98.022511)

I. INTRODUCTION

The precision spectroscopy of isolated molecules is making strong advances thanks to novel techniques of trapping, cooling, and manipulation. One family of molecules, the molecular hydrogen ions, is particularly attractive because their transition frequencies can be calculated *ab initio* with a precision that challenges current experimental approaches [1].

The comparison of theoretical with experimental frequencies allows extracting the values of certain fundamental constants, such as the electron-to-proton mass ratio and the Rydberg constant [2–5]. In this endeavor, one is faced with the problem that the theoretical frequencies are not just given by the solution of the Schrödinger three-body problem, but include relativistic and QED contributions, as well as spin-dependent contributions. In addition, the experimentally measured frequencies are perturbed by external fields whose strength cannot always be determined accurately enough.

The spin-dependent contributions can be calculated and, in fact, the accuracy of the calculation has made impressive progress in recent years [6]. Nevertheless, it will become harder to push the accuracy further. Thus it is worthwhile to consider whether there are experimentally viable approaches to determine the (not directly observable) spin-averaged transition frequency from a *combination* of measured transition frequencies. The solution to this query makes use of the mathematical property of a class of Hamiltonians, the tracelessness. In atomic physics, this approach is well known; here the computed “center of gravity” of the fine structure or of the hyperfine structure of a level is often considered. In the field of metrology it is, for example, used to characterize the helium isotope shift [7].

We further consider an important subset of systematic shifts affecting the transition frequencies. When the shifts are small, so that first-order and second-order perturbation is applicable, their mathematical structure is such that an appropriate average over them vanishes exactly. This principle was recently implicitly used by Karr *et al.* [8] in an analysis of promising transitions for the precision spectroscopy of H_2^+ . Here we illuminate the principle from a broader perspective and show the close relationship to the concept of the spin-averaged transition frequency determination.

Composite frequencies being at the focus of the present work, it complements our previous discussion [9], in which we considered the combination of different rovibrational transitions for the cancellation of systematic shifts. Here, individual rovibrational transitions are considered.

The paper is structured as follows. In Sec. I we derive cancellation conditions from the tracelessness of the Hamiltonian. In Sec. II it is shown that they lead to the possibility of determining the spin-averaged frequency via the combination of a set of electric-dipole transitions. In Sec. III the conditions for cancellation of three types of systematic shifts are derived: linear Zeeman shift, quadratic Zeeman shift, and electric quadrupole shift. A fourth systematic shift, the Stark shift, can be partially canceled, since its tensor part is canceled whenever the quadrupole shift is. In Sec. IV we state how spin contributions and shifts can be simultaneously canceled. In Sec. V we apply the general discussion of spin-structure cancellation to the molecular hydrogen ions H_2^+ and HD^+ . In Sec. VI we show that an obvious extension leads to cancellation of the linear Zeeman shift as well. Further shifts can also be canceled by including more transitions. Subsequently, the general method from Sec. IV is applied. For each approach, the systematic shifts stemming from the uncanceled perturbations are evaluated and discussed, leading to estimates for the achievable residual shifts. In Sec. VII

*Corresponding author: step.schiller@hhu.de

we discuss a more efficient approach for canceling both spin-structure and systematic shifts. Section VIII draws the conclusions.

II. CANCELLATIONS: ELEMENTARY CONSIDERATIONS

Consider a complete set $\{|\psi_i\rangle\}$ of basis states, where i denotes the set of quantum numbers uniquely identifying a state, and a generic traceless operator H^1 . The traceless property implies

$$0 = \text{Tr}(H^1) = \sum_i \langle \psi_i | H^1 | \psi_i \rangle. \quad (1)$$

The trace can be evaluated in any basis. In particular, we can choose a set of basis states that diagonalizes the operator H^1 , its eigenstates.

Consider now the operator H^1 to be a contribution to the total Hamiltonian H . The tracelessness of H^1 then yields a relationship between the energy contributions E_ξ^1 :

$$0 = \text{Tr}(H^1) = \sum_\xi d_\xi E_\xi^1, \quad (2)$$

where d_ξ is the degeneracy factor for those states having the same energy contribution E_ξ^1 , and ξ denotes the set of quantum numbers identifying the different *energy levels*. The vanishing of the trace implies the existence of positive- and negative-energy contributions.

Often, one is concerned with states that are characterized by a total angular momentum quantum number, J , and a magnetic quantum number, J_z , in addition to other quantum numbers n . We may choose these states as basis states. In the case of rotational invariance of the Hamiltonian H^1 , its expectation values are independent of J_z . In this case the above expression takes the form

$$0 = \text{Tr}(H^1) = \sum_{n,J} (2J+1) \langle \psi_{n,J} | H^1 | \psi_{n,J} \rangle, \quad (3)$$

where $2J+1$ is the magnetic degeneracy factor.

The typical situation in atomic and molecular physics is that the system is described by a total Hamiltonian H which is the sum of a “dominant” term, H^0 (spin-independent or spin-averaged), and several traceless perturbations, each denoted by H^j . The energy of an eigenstate $|\psi_k\rangle$ of the total Hamiltonian is approximated by first-order perturbation theory,

$$\begin{aligned} E_k &= E_k^0 + \sum_j E_k^j \\ &= \langle \psi_k^0 | H^0 | \psi_k^0 \rangle + \sum_j \langle \psi_k^0 | H^j | \psi_k^0 \rangle. \end{aligned} \quad (4)$$

The expectation values are taken for the unperturbed states $|\psi_k^0\rangle$, the eigenstates of the dominant Hamiltonian H^0 . In fact, the quantum numbers for a state k can be written more explicitly as p, m , where p refers to the set describing the state space of the dominant Hamiltonian, and m to the space of the perturbation Hamiltonian. The trace condition is then

$$0 = \text{Tr}(H^j) = \sum_m \langle \psi_{p,m}^0 | H^j | \psi_{p,m}^0 \rangle. \quad (5)$$

When we perform spectroscopy, we measure energy differences $E_{k'} - E_k = E_{p',m'} - E_{p,m}$. The question we pose is whether a combination of such energy differences, provided

they are experimentally accessible, allows one to determine the dominant contribution $E_{k'}^0 - E_k^0$, which may be of interest. To this end, we consider a linear combination of transition frequencies, the “traceless” frequency f_t , of the form

$$h f_t(p \rightarrow p') = \sum_{m,m'} \alpha(p', m'; p, m) (E_{p',m'} - E_{p,m}), \quad (6)$$

with (positive or negative) weights α . This ansatz is successful, if the following three conditions hold.

(I) All transition frequencies $h f(k \rightarrow k') = E_{p',m'} - E_{p,m}$ are experimentally measurable (necessarily, the transitions must be allowed by selection rules).

(II) $\sum_{m'} \alpha(p', m'; p, m) = 1/\mathcal{N}$ is satisfied for all possible values m .

(III) $\sum_m \alpha(p', m'; p, m) = 1/\mathcal{N}'$ is satisfied for all possible values m' .

Here $\mathcal{N} = \sum_m 1$ is the total number of states for given p , etc. (II) and (III) simply mean that in the set of selected transition frequencies each initial state should occur with equal total weight $1/\mathcal{N}$ and each final state should occur with equal total weight $1/\mathcal{N}'$.

Then, Eq. (6) simplifies to

$$\begin{aligned} h f_t(p \rightarrow p') &= \sum_{m,m'} \alpha(p', m'; p, m) E_{p',m'} \\ &\quad - \sum_{m,m'} \alpha(p', m'; p, m) E_{p,m} \\ &= \sum_{m'} (1/\mathcal{N}') \left(E_{p'}^0 + \sum_j E_{p',m'}^j \right) \\ &\quad - \sum_m (1/\mathcal{N}) \left(E_p^0 + \sum_j E_{p,m}^j \right) \\ &= \sum_{m'} (1/\mathcal{N}') E_{p'}^0 - \sum_m (1/\mathcal{N}) E_p^0 \\ &= E_{p'}^0 - E_p^0, \end{aligned} \quad (7)$$

where we have made use of the tracelessness, $0 = \sum_{m'} E_{p',m'}^j = \sum_m E_{p,m}^j$.

III. CANCELLATION OF SPIN-STRUCTURE CONTRIBUTIONS

Generally, the effective spin Hamiltonian, comprising fine structure, hyperfine structure, and interaction of the electron(s) with the nuclear quadrupole moment, may be expressed as a sum of traceless operators,

$$H^{\text{spin}} = \sum_j \mathcal{E}_j (T_a^{(k)} \cdot U_b^{(k)}), \quad (8)$$

where $T_a^{(k)}$ and $U_b^{(k)}$ are some irreducible tensors of spin or orbital operators and the dot is a tensor scalar product

$$T_a^{(k)} \cdot U_b^{(k)} = \sum_\mu (-1)^\mu T_{a,\mu}^{(k)} U_{b,-\mu}^{(k)}.$$

A first example is the spin-orbit interaction $\mathcal{E}_j(\mathbf{N} \cdot \mathbf{s}_j)$, where \mathbf{N} is the operator of the total orbital angular momentum and \mathbf{s}_j is the spin operator of particle j . A second example is the

tensor quadrupole interaction,

$$E_j[\mathbf{N}^2(\mathbf{s}_k \cdot \mathbf{s}_l) - 3[(\mathbf{N} \cdot \mathbf{s}_k)(\mathbf{N} \cdot \mathbf{s}_l) + (\mathbf{N} \cdot \mathbf{s}_l)(\mathbf{N} \cdot \mathbf{s}_k)]].$$

This form is provided by the spin-dependent part of the Breit-Pauli Hamiltonian. Higher-order corrections enter either as corrections to the coefficients of the already existing interactions, or as new, more complicated irreducible tensor (traceless) interactions, or they contribute to the spin-averaged part of the energy of a state.

If the system is composed by three particles with spin, we introduce the two-particle spin operator $\mathbf{F} = \mathbf{s}_1 + \mathbf{s}_2$, and the three-particle spin operator $\mathbf{S} = \mathbf{F} + \mathbf{s}_3$, which generally do not commute with the total Hamiltonian. The total angular momentum, $\mathbf{J} = \mathbf{S} + \mathbf{N}$, does commute with H , and J, J_z are good quantum numbers. As basis states we can take pure angular momentum states or the eigenstates of the total Hamiltonian $H = H^0 + H^{\text{spin}}$. In both cases we can denote them by $|p, F S J J_z\rangle$. In the latter case, the numbers F, S are chosen as the integers closest to the numbers \bar{F}, \bar{S} resulting from the expectation values $\langle \mathbf{F}^2 \rangle = \hbar^2 \bar{F}(\bar{F} + 1)$ and $\langle \mathbf{S}^2 \rangle = \hbar^2 \bar{S}(\bar{S} + 1)$ in the given state. In the absence of magnetic field, the eigenstates are degenerate in J_z . We denote by $E_{p,FSJ}^{\text{spin}}$ the perturbation energy of state $|p, F S J J_z\rangle$ due to H^{spin} .

The following sum rule holds for the traceless spin Hamiltonian:

$$\sum_{FSJ} (2J + 1) E_{p,FSJ}^{\text{spin}} = 0. \quad (9)$$

The sum is over all spin states. The proof is straightforward because it is fulfilled for each individual term in Eq. (8) [10].

We now consider transitions and show how the traceless frequency Eq. (6) can be implemented. A transition frequency between two particular spin states of two rovibrational levels is

$$h f(p F S J \rightarrow p' F' S' J') = E_{p'}^0 - E_p^0 + E_{p',F'S'J'}^{\text{spin}} - E_{p,FSJ}^{\text{spin}}. \quad (10)$$

We consider here $E1$ transitions connecting equal initial spin and final spin states with equal spin configurations ($F = F', S = S'$). They have the largest transition dipole moments [16] and are therefore called “favored”. Other transitions are strongly suppressed. Although F, S do not change in favored transitions, the values must nevertheless be stated, allowing to uniquely identify the state.

The following quantity vanishes:

$$\sum_{(FSJ) \rightarrow (FSJ')} (2J' + 1)(E_{p',FSJ'}^{\text{spin}} - E_{p,FSJ}^{\text{spin}}) = 0, \quad (11)$$

where the sum is over all favored $E1$ transitions between levels p and p' .

The proof is as follows. The $E1$ selection rule is $J \rightarrow J' = J, J \pm 1$. If $J = 0$, then $J' = 1$.

We use the obvious relation

$$\begin{aligned} \sum_{J=J, J \pm 1} (2J' + 1) &= [2(J + 1) + 1] + (2J + 1) \\ &+ [2(J - 1) + 1] = 3(2J + 1), \end{aligned}$$

or for $J = 0: 3(2J + 1) = 3 = (2J' + 1)$. That proves that the left-hand side (LHS) of Eq. (11) may be written as

$$\sum_{(FSJ')} (2J' + 1) E_{p',FSJ'}^{\text{spin}} - 3 \sum_{(FSJ)} (2J + 1) E_{p,FSJ}^{\text{spin}},$$

which vanishes on account of tracelessness, Eq. (9). Thus the traceless frequency constructed from all favored $E1$ transition frequencies,

$$\begin{aligned} f_t^{\text{spin}} &= \mathcal{M}^{-1} \sum_{(FSJ) \rightarrow (FSJ')} (2J' + 1) f(p F S J \rightarrow p' F S J') \quad (12) \\ &= (E_{p'}^0 - E_p^0)/h, \quad (13) \end{aligned}$$

is equal to the spin-averaged transition frequency $f^0(p \rightarrow p')$. Here, $\mathcal{M} = \sum_{(FSJ) \rightarrow (FSJ')} (2J' + 1)$ is a normalization factor. In Sec. VIB below, we show an example of the set of transitions that are included in the sum.

When $E1$ transitions do not exist, the treatment must be modified; see Sec. VIC below.

IV. CANCELLATION OF SYSTEMATIC SHIFTS

A. Linear Zeeman shift and electric quadrupole shift:

A simple model

We now consider a simple example: a quantum system possessing angular momentum \mathbf{J} and an electric quadrupole moment, exposed to an external magnetic field \mathbf{B} pointing along the z axis and to an external electric-field gradient V_{zz} . Assume the magnetic and electric quadrupole perturbation Hamiltonian to be of the form

$$H_p^1 = -\mu_B g(p) \mathbf{J} \cdot \mathbf{B} + d(p) V_{zz} (\mathbf{J}^2 - 3J_z^2). \quad (14)$$

Both contributions are traceless. The coefficients g and d may in general differ in different states p of the unperturbed Hamiltonian H^0 . The state quantum numbers summarized by p include J , which is assumed fixed in this example. The angular momentum projection quantum number J_z now plays the role of the quantum number m . The linear Zeeman (LZ) shift and the electric quadrupole (EQ) shift are computed in first-order perturbation theory. The tracelessness of H_p^1 is expressed by the sum rule,

$$\begin{aligned} \sum_{J_z} E_{p,J_z}^1 &= \sum_{J_z} -\mu_B g(p) J_z |\mathbf{B}| \\ &+ d(p) V_{zz} [J(J + 1) - 3J_z^2] = 0, \quad (15) \end{aligned}$$

which holds independent of the specific values of J (integer or half-integer), g, d (and thus of the specific level p) and of the field strengths $|\mathbf{B}|$ and V_{zz} .

The following examples illustrate how to include this sum rule into the traceless frequency. In Figs. 1(a)–1(c) we show schematically some energy levels of the total Hamiltonian, a lower level p having $J = 0, 1$, or 2 , and an upper level p' having $J' = 1, 2$, or 3 . The energy of a state is $E_p^0 + E_{p,J_z}^1$. A number of electric dipole ($E1$) transitions between the two levels, obeying the selection rules $\Delta J = J' - J = 0, \pm 1, \Delta J_z = 0, \pm 1$, have been selected and assigned specific weights $\alpha(J', J'_z; J, J_z)$ satisfying the conditions (II) and (III). These weights can easily be found by solving appropriate conditions. In the case Fig. 1(b), the nine transitions $J_z \rightarrow J'_z$,

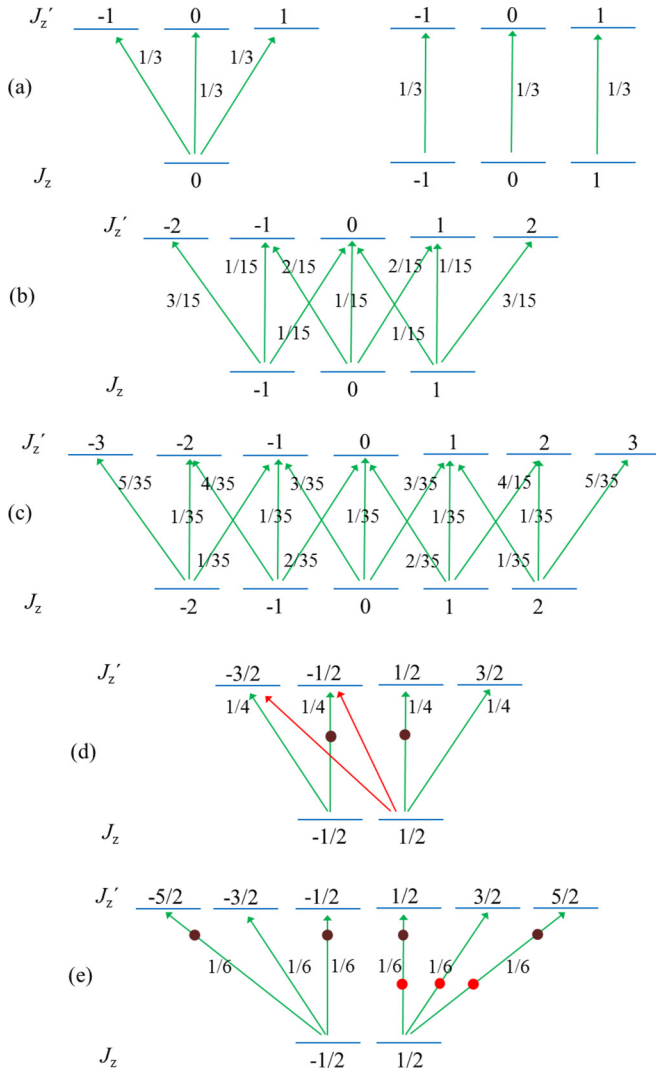


FIG. 1. Schematic energy diagrams comprising a lower level having angular momentum J and an upper level J' . Panels (a)–(e) show different cases (J, J') . The green arrows denote transitions between specific magnetic sublevels J_z, J'_z to be measured. Each assigned coefficient α multiplies the corresponding transition frequency so that in the weighted sum f_l^1 the external-field perturbations average to zero. (a)–(d) $E1$ or $E2$ transitions; (e) $E2$ transitions. The case $J = 2, J' = 2$ is not shown; it can easily be obtained by generalization of (a), right-hand side. The coefficients for the cases where $J > J'$ are obtained from the above cases by symmetry. Red arrows, brown and red disks: see text.

which altogether address every state of the lower level with the same weight (1/3) and every state of the upper level with the same weight (1/5), serve to null the effect of four interactions, proportional to $g(p, J)|\mathbf{B}|$, $g(p', J')|\mathbf{B}|$, $d(p, J)V_{zz}$, and $d(p', J')V_{zz}$,

$$h f_l^1 = h \sum_{J_z, J'_z} \alpha(J', J'_z; J, J_z) f(p, J_z \rightarrow p', J'_z) = E_{p'}^0 - E_p^0.$$

The specific cases (a)–(c) can easily be generalized to higher values of J and $J' = J + 1$.

The panels (d) and (e) in the same figure show cases of half-integer angular momenta, $J = 1/2, J' = 3/2, 5/2$, and

electric-quadrupole ($E2$) transitions. A suitable set of transitions, satisfying the selection rule for $E2$ transitions, and appropriate weights are found by inspection. For example, panel (d) shows the case where the measurement of a total of four individual transitions $f(p, J_z \rightarrow p', J'_z)$ (green arrows) allows canceling the effect of Zeeman and EQ interactions in both the lower ($J = 1/2$) and upper ($J' = 3/2$) level, defined by four interactions. In panel (e) J' is larger, and now six transitions are required for canceling again four interactions. However, in these particular cases having $J = 1/2$, the EQ interaction in the lower level vanishes, so effectively only three interactions are canceled. The cases $J \rightarrow J' = J$ are trivial; therefore, only one example is shown in panel (a), right-hand side.

We emphasize that the presented scheme for nulling the effects of the Zeeman and quadrupole shifts is not unique. Other types of combinations of transition frequencies are possible. Specifically, for H_2^+ , Karr *et al.* [8] have considered a combination of frequencies involving two different angular momentum subspaces in one of the two levels (see also below). Such other combinations can be more efficient, requiring a smaller number of transitions to be measured.

B. Zeeman shift and electric quadrupole shift: Realistic case

The EQ interaction between an external field gradient and the electronic plus nuclear charge distribution has the form

$$H^{\text{EQ}}(p) \propto (\mathbf{N} \otimes \mathbf{N})^{(2)},$$

where the RHS is an irreducible tensor operator of rank 2. This Hamiltonian is traceless. Its effects are evaluated in first-order perturbation theory, due to the smallness of the field gradient occurring in experiments. The Hamiltonian can be replaced by [11]

$$H^{\text{EQ}}(p) \propto \mathbf{J}^2 - 3\hat{J}_z^2.$$

The first-order energy shifts of a given state $(p, F S J)$ are $E_{p, F S J}^{\text{EQ}} \propto J(J+1) - 3J_z^2$, the same as for the simple model above.

The Stark shift arises from light fields and trap fields. In general, it has a scalar, vector, and tensor contribution [12] [see Eq. (5) in Ref. [13] for the formal expression for the static Stark shift]. The tensor contribution has the same dependence on the angular momentum quantum numbers as the EQ shift. Therefore, cancellation of EQ shift implies cancellation of the tensor Stark shift.

In real systems, the interaction with the external magnetic field is typically not of the form Eq. (14). For a three-particle system, in general,

$$H^{\text{mag}}(p) = -\mu_B(g_1(p)\hat{s}_{1,z} + g_2(p)\hat{s}_{2,z} + g_3(p)\hat{s}_{3,z} + g_L(p)\hat{N}_z)B_z.$$

This Hamiltonian is traceless, and furthermore commutes with \hat{J}_z . We can take advantage of the structure of the magnetic shifts that occur in first order and in second order in B_z and incorporate them into the traceless frequency.

In first-order perturbation theory,

$$E_{p, F S J J_z}^{\text{LZ}} = \langle p, F S J J_z | H^{\text{mag}}(p) | p, F S J J_z \rangle \propto J_z.$$

The LZ shift is proportional to J_z by virtue of the Wigner-Eckhart theorem.

At today's desired precision levels, it is insufficient to consider only the LZ shift. It is necessary to also consider the quadratic Zeeman (QZ) shift, which according to second-order perturbation theory is

$$E_{p,FSJJ_z}^{\text{QZ}} = \sum_{F'S'J' \neq FSJ} \frac{|\langle p, F'S'J'J_z | H^{\text{mag}}(p) | p, FSJJ_z \rangle|^2}{E_{p,FSJ}^0 - E_{p,F'S'J'}^0} \quad (16)$$

for a state $|p, FSJJ_z\rangle$. The sum goes over all spin-structure states ($F'S'J'$) but is limited to states in the same level p . Also, $J'_z = J_z$ since H^{mag} commutes with the operator \hat{J}_z . Because the denominator is antisymmetric under "state exchange" ($FSJ \leftrightarrow F'S'J'$), while the numerator is symmetric, it follows that for any given J_z

$$\sum_{FSJ} E_{p,FSJJ_z}^{\text{QZ}} = 0. \quad (17)$$

The sum over the quadratic Zeeman shifts of all spin states in a given rovibrational level p and having a given J_z is zero. This sum rule does not contain any degeneracy factor since J_z is fixed.

Note that there exists only one state having $J_z = J_{\text{max}} = F + S + N$ and one having $J_z = -J_{\text{max}}$ (stretched states). These states therefore do not exhibit a QZ shift.

V. COMBINING SPIN-STRUCTURE CANCELLATION WITH SYSTEMATIC SHIFT CANCELLATION

The standard situation in the description of the molecular hydrogen ions is to consider the spin-structure contributions and systematic shifts for each rovibrational level p , independent of the others. This is a good approximation because both types of contributions are very small compared to the energy difference to neighboring rotational levels of the same vibrational level and even smaller compared to the energy difference to neighboring vibrational levels. The Hamiltonians H^j of the perturbations therefore are effective Hamiltonians, i.e., they contain parameters that depend on the concrete level p : $H^j = H^j(p)$. Given an arbitrary basis of spin states q for the particular level p , one can set up the Hamiltonian matrix

$$H_{q',q}^{\text{pert}}(p) = \langle q' | H^{\text{spin}}(p) + H^{\text{mag}}(p) + H^{\text{EQ}}(p) | q \rangle, \quad (18)$$

and diagonalize it in order to find the eigenstates m and the eigenenergies $E_{p,m}^{\text{pert}}$. Because each contribution in $H^{\text{pert}}(p)$ is traceless, we have the sum rule

$$\sum_q H_{q,q}^{\text{pert}}(p) = \sum_m E_{p,m}^{\text{pert}} = 0. \quad (19)$$

We emphasize that this sum rule refers to the "exact" total perturbation shifts, to all orders in any perturbation parameter, e.g., the magnetic-field strength or electric-field gradient strength.

Since it is permissible to consider various orders of a particular perturbation, e.g., the linear Zeeman shift and the quadratic Zeeman shift, there necessarily follow separate sum rules for these orders. Some of these have been already given above. Indeed, for practical reasons it is useful to take this point of view: in precision spectroscopy, one strives experimentally to make as many of the perturbations as small as possible, so that the dominant contribution to H^{pert} is the spin structure Hamiltonian H^{spin} . The other perturbations are then treated in

first-order perturbation theory with respect to the eigenstates of H^{spin} , and only occasionally also second-order perturbation theory is applied. The advantage of this approach is that the perturbation energy of a state (p, m) can then be written as a sum of contributions, and the total energy is

$$E_{p,m} = E_p^0 + E_{p,m}^{\text{spin}} + E_{p,m}^{\text{LZ}} + E_{p,m}^{\text{QZ}} + E_{p,m}^{\text{EQ}}.$$

Here, m corresponds to $FSJJ_z$. The spin interaction is treated exactly (by diagonalization), while the Zeeman interaction is treated to second-order perturbation theory (LZ, QZ), and the EQ interaction only to first-order perturbation theory. All perturbations come with their own sum rules, which have been presented above. They do differ in form; therefore

(i) The LZS can be nulled, for any particular FSJ , by summing over all J_z , or pairwise over J_z and $-J_z$.

(ii) The EQS can be nulled, for any particular FSJ , by summing over all J_z .

(iii) The QZ shift can be nulled, for any fixed J_z , by summing over all states FSJ containing this Zeeman state.

(iv) The spin-structure contributions can be nulled by summing over all states $FSJJ_z$, or over all states FSJ with $J_z = 0$.

Although these sum rules differ, not surprisingly they can nevertheless be incorporated *together* in a traceless frequency as in Eq. (6), by defining

$$h f_t^{\text{pert-free}}(p \rightarrow p') = \sum_{m,m'} \tilde{\alpha}(p', m'; p, m) (E_{p',m'} - E_{p,m}), \quad (20)$$

A sum over all possible transitions $m \rightarrow m'$ is taken, with the following restrictions.

(1) Only those $FSJ \rightarrow F'S'J'$ transitions are included that allow the spin-structure cancellation as in the case of absence of external fields. Depending on the particular transition $p \rightarrow p'$, either each upper state $F'S'J'$ is associated with one lower state FSJ only, or vice versa (for the whole set of lower states). Here one disregards the concrete Zeeman components.

(2) For each of these transitions, one measures the $J_z \rightarrow J'_z$ components as shown in Fig. 1, multiplies the components' frequencies with the weights indicated, and further multiplies each with the factor $\alpha = (2J' + 1)/\mathcal{N}'$. The resulting weights are the $\tilde{\alpha}$ of Eq. (20).

$f_t^{\text{pert-free}}$ is free from LZ shift and EQ shift by construction, already at the level of each individual transition $FSJ \rightarrow F'S'J'$ because, according to Fig. 1, (i) equal weight are given to the $J_z \rightarrow J'_z$ and $-J_z \rightarrow -J'_z$ transitions and (ii) all J_z and J'_z substates contribute with equal weight. Furthermore, $f_t^{\text{pert-free}}$ is free of spin structure because of the definition of weights as given in (2). Finally, with this procedure, the total QZ shift also cancels: because each J'_z state enters $f_t^{\text{pert-free}}$ with the same (total) weight $1/(2|J'_z| + 1)\mathcal{N}'$ and similarly for each J_z state, Eq. (17) applies. As an example, consider the $J'_z = -1$ states in Figs. 1(a)–1(c): in each panel, their total weight is always 1/3. Thus

$$h f_t^{\text{pert-free}}(p \rightarrow p') = E_{p'}^0 - E_p^0. \quad (21)$$

The traceless frequency defined in this way is equal to the unperturbed (spin-averaged) frequency $f^0(p \rightarrow p')$. This scheme is generally applicable, but variations can be more

efficient in terms of minimizing the number of transitions to be measured, and will be discussed below.

A. Special cases

For systems with integer J , there exist the $J_z = 0 \rightarrow J'_z = 0$ Zeeman components. Measuring only these for the traceless frequency leads to zero total LZ shift.

Similarly, for systems with half-integer spin, the two Zeeman components $J_z = 1/2 \rightarrow J'_z = -1/2$ and $J_z = 1/2 \rightarrow J'_z = -1/2$ exist. In the mean frequency of these two components the LZ effect vanishes, for each hyperfine transition $F S J \rightarrow F' S' J'$.

Such traceless frequencies will have a well-defined, nonzero EQ shift and QZ shift. We shall take this up again in Sec. VII A.

VI. APPLICATION TO THE MOLECULAR HYDROGEN IONS

A. Motivation

The scope of the following discussion is to present in a detailed manner the application of the traceless frequency to the elimination of the spin-dependent energies in H_2^+ and HD^+ .

Consider a single spin component $m \rightarrow m'$ within the spin structure of a transition between the rovibrational levels $p : (v, N) \rightarrow p' : (v', N')$ (v : vibrational quantum number; N : rotational quantum number). The lower and upper spin states are enumerated by quantum numbers denoted collectively as m and m' . The frequency of an individual transition is computed as a sum of two contributions:

$$f(v, N, m \rightarrow v', N', m') = f^{\text{spin-avg}}(v, N \rightarrow v', N') + f^{\text{spin}}(v, N, m \rightarrow v', N', m'). \quad (22)$$

The spin-averaged frequency $f^{\text{spin-avg}}$ (corresponding to f^0 above) depends only on v, N, v' , and N' . Currently, it can be computed with a fractional inaccuracy due to theory at the 1×10^{-11} level, for both vibrational [1] and rotational transitions [5]. The second contribution is the spin-structure (hyperfine) shift $h f^{\text{spin}} = E_{vN,m}^{\text{spin}} - E_{v'N',m'}^{\text{spin}}$ due to spin interactions. The effective spin Hamiltonian H^{spin} has been derived within the Breit-Pauli approximation [14,15]. It contains a set $\{\mathcal{E}_q\}$ of (v, N) -dependent coefficients. The number of coefficients in the set is up to nine for HD^+ and up to five for H_2^+ . The inaccuracy of the *ab initio* calculation of the set of coefficients is the dominant source of the theoretical inaccuracy of f^{spin} , at present [6].

In general, the spin energies of a state are obtained numerically by diagonalizing the spin Hamiltonian. For HD^+ , only a few particular states have energies expressible in explicit form. This is the case for the stretched states (states of maximum total angular momentum, $J_{\text{max}} = N + 2$, and maximum total angular momentum projection, $|J_z| = J_{\text{max}}$), for which (see Eq. (6) in [16])

$$E_{vN}^{\text{spin}}(F = 1, S = 2, J = N + 2, J_z = \pm J)/h = \mathcal{E}_4/4 + \mathcal{E}_5/2 + (\mathcal{E}_1 + \mathcal{E}_2 + 2\mathcal{E}_3 + \mathcal{E}_6 + 2\mathcal{E}_7 + 2\mathcal{E}_8 + \mathcal{E}_9)N/2 - (2\mathcal{E}_6 + 4\mathcal{E}_7 + 4\mathcal{E}_8 + 2\mathcal{E}_9)N^2/2. \quad (23)$$

This expression is helpful in showing how any theoretical inaccuracy of the \mathcal{E}_q will affect the theoretical inaccuracy of the overall transition frequency f .

Since the present considerations are independent of the particular vibrational levels, we shall often omit the mention of v, v' in the state designations when they are not essential.

B. The molecular ion HD^+

Each state of HD^+ is uniquely defined by the quantum numbers $p : (v, N)$ and $m : (F S J J_z)$. As introduced in Sec. III, F is (approximate or exact) spin of the electron-proton pair, S is the (approximate or exact) total spin of the three particles, and J is the (exact) total angular momentum quantum number of the molecule.

Before proceeding we note that the tracelessness property of the Breit-Pauli interaction Hamiltonian and the sum rule for the QZ shifts are relationships that can be verified on computed energy shifts in order to check for correctness of the computation [17].

Let us initially ignore the external-field shifts. A general argument allows us to find the weights α for the traceless frequency. For simplicity, we assume zero magnetic field and zero electric-field gradient, so that the states are degenerate in J_z , and we omit this quantum number in the following. The appropriate type of transitions are electric dipole ($E1$), which allow $J \rightarrow J' = J - 1, J, J + 1$, and $\Delta N = \pm 1$. Strong $E1$ transitions are those for which the conditions $\Delta F = 0$ and $\Delta S = 0$ are fulfilled.

For concreteness, we discuss the case of transitions from a lower level $N = 0$ to an upper level $N' = 1$. There is no restriction on v and v' . Two transitions of this type have already been measured with 10^{-9} -level fractional inaccuracy [3,5]. One relevant case is the rotational transition between the two lowest-energy rovibrational levels, $(v = 0, N = 0) \rightarrow (v' = 0, N' = 1)$, with $f^{\text{spin-avg}} \simeq 1.3$ THz. The spin structure of this transition has been discussed previously [5,16,18] and Fig. 2 reports the detailed energy diagram with the actual spin energies E^{spin} .

Each spin state $|N = 0, F S J\rangle$ of the lower level having $S \neq 0$ can be excited to three spin states (forming a ‘‘spin group’’) of the upper level, namely $|N' = 1, F S J - 1\rangle$, $|1, F S J\rangle$, and $|1, F S J + 1\rangle$, by favored (strong) transitions. To these transitions we assign weights proportional to the degeneracies of the respective upper states, $\alpha(J; J') = (2J' + 1)/N'$. In the traceless frequency sum, each state of the upper level occurs once and therefore the total contribution of the spin-averaged energies of the upper states yields $E_{v'N'}^{\text{spin-avg}}/h$. The total contribution of their spin energies, however, averages to zero because of the tracelessness of the spin Hamiltonian.

The state $|N = 0, F = 1, S = 0, J = 0\rangle$ is special: it has only a single strong transition to the state $|N' = 1, F' = 1, S' = 0, J' = 1\rangle$ (green line in the figure). Nevertheless, the above weight assignment is suitable.

As a consequence of the above weight assignment, the total weight of each lower spin state in the sum is $\alpha(J; J - 1) + \alpha(J; J) + \alpha(J; J + 1) = 3(2J + 1)/N'$, since three transitions start from each state. This total weight naturally turns out to be the degeneracy of the lower state, up to a constant factor. Here again, $N' = 2 \times 2 \times 3 \times (2N' + 1) = 36$ is the

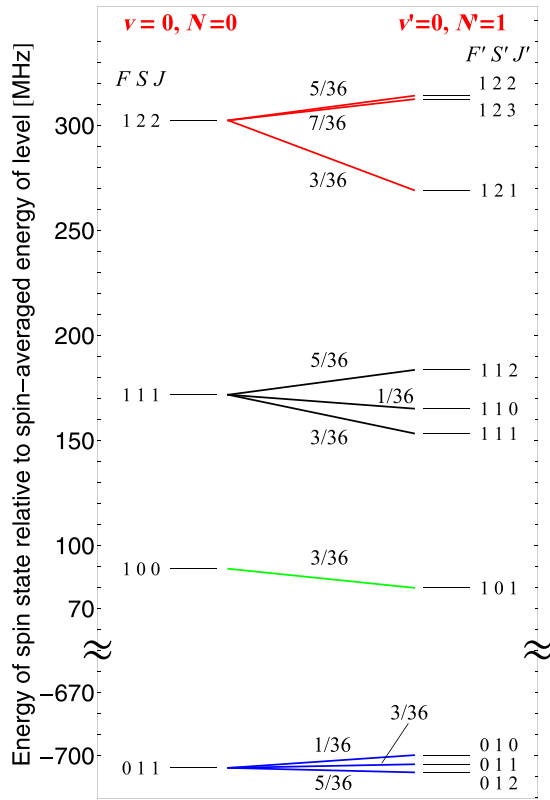


FIG. 2. Energies $E_{vN,m}^{\text{spin}}$, $E_{v'N',m'}^{\text{spin}}$ of the spin states of HD^+ relevant for the fundamental rotational transition ($v = 0, N = 0$) \rightarrow ($v' = 0, N' = 1$). The colored lines indicate the transitions to be measured in order to compute the traceless transition frequency. The numbers above the colored lines are the weights α . For both levels, the zero of the vertical scale corresponds to the respective spin-averaged energy $E_{vN}^{\text{spin-avg}}$. Adapted from Ref. [18].

number of states in the upper level. The special state $|0, F = 1, S = 0, J = 0\rangle$ is again taken into account correctly, even if only a single transition starts from it. The total contribution of the four lower states yields

$$\sum_{FSJ \in \{011, 100, 111, 122\}} [3(2J + 1)/\mathcal{N}'] E_{0N}^{\text{spin-avg}}/h$$

$$= (3\mathcal{N}/\mathcal{N}') E_{0N}^{\text{spin-avg}}/h \quad (24)$$

$$= E_{0N}^{\text{spin-avg}}/h. \quad (25)$$

Here, the number of states in the lower level is $\mathcal{N} = 12$.

Explicitly, the traceless frequency is (with the arbitrary vibrational quantum numbers v, v' reintroduced)

$$f_t^{\text{spin}} = \sum_{FSJ \rightarrow F'S'J'} [(2J' + 1)/\mathcal{N}']$$

$$\times f(v, 0, F S J \rightarrow v', 1, F' S' J')$$

$$= f^{\text{spin-avg}}(v, 0 \rightarrow v', 1). \quad (26)$$

The summation is limited to the 10 strong (favored) $E1$ transitions (the colored lines in Fig. 2). The traceless frequency eliminates the contributions from 11 spin-structure coefficients (nine of the upper level and two of the lower level), for any choice of vibrational levels v, v' .

Note that for given v, N, v', N' , the transition frequencies $f(v, N, m \rightarrow v', N', m')$ lie in a range of several 10 MHz, and thus only a single radiation source is sufficient for their measurement.

Transitions between levels whose rotational quantum numbers N, N' are both nonzero require a generalization of Eq. (26). The situation is now richer in the sense that in the lower level there will typically be more than just one spin state J for a given quantum number pair (F, S) (see the right-hand side of Fig. 2 for the case $N = 1$). This situation can easily be treated by setting up a set of equations for the unknown weights α , requiring that the sum of weights of the strong spin transitions connecting to any particular state m or m' be equal to the normalized Zeeman degeneracy of that state, $[2J(m) + 1]/\mathcal{N}$ or $[2J(m') + 1]/\mathcal{N}'$, respectively. The set contains one equation for every state in the lower and in the upper level. The solution of the set of equations shows that for a $N = 1 \rightarrow N' = 2$ transition, 18 spin transitions (5, 1, 5, 7 for the four spin groups, respectively) must be measured, and for $N \geq 2 \rightarrow N' = N + 1$ the number increases to 20 spin transitions (5, 1, 5, 9 for the four spin groups, respectively). It is found that not all strong transitions necessarily must contribute to f_t . The overall result is that, in the traceless frequency, the influence of 18 coefficients of the Breit-Pauli interaction is canceled.

C. The molecular ion H_2^+

H_2^+ exhibits some important differences compared to HD^+ because it is homonuclear. States are denoted by $|v, N, I, F, J\rangle$, where I is the (exact) total nuclear spin quantum number and F is the (approximate or exact) total particle spin angular momentum quantum number.

Rovibrational levels with even $N = 0, 2, 4, \dots$ are “para” levels with zero total nuclear spin $I = 0$. The total particle spin angular momentum is $F = 1/2$. The spin Hamiltonian reduces to the spin-rotation interaction, $H^{\text{spin}} = c_e(\mathbf{s}_e \cdot \mathbf{N})$. Rovibrational levels (v, N) are therefore split into two if $N \geq 2$. The energies of the $J = N - 1/2$ and $J = N + 1/2$ levels are $-(N + 1)c_e/2$ (if $N \geq 2$) and $Nc_e/2$, respectively.

In the case of odd $N = 1, 3, \dots$ the molecule is in an “ortho” ($I = 1$) state and the total particle spin angular momentum is $F = 1/2$ or $F = 3/2$. The number of spin levels is higher, 5 for $L = 1$ and 6 for $L = 3, 5, \dots$ Figure 3 shows the spin structure of the lowest rovibrational levels.

As a homonuclear molecule, H_2^+ cannot be interrogated by one-photon electric-dipole ($E1$) transitions. Therefore, compared to the HD^+ case, an adapted discussion is required. Accessible transitions are two-photon transitions and electric-quadrupole ($E2$) transitions, already discussed in detail [19,20]. We consider here only $E2$ transitions, because they show greater potential than two-photon transitions. Figure 3 shows $E2$ transitions relevant for the following discussion. The crucial issue are the selection rules for $E2$ transitions. The total molecular angular momentum can change by $\Delta J = 0, \pm 1, \pm 2$. In particular, the fact that $\Delta J = 0$ are allowed transitions is important in the context of the present discussion. Such transitions also have an unsuppressed strength, if $\Delta F = 0$ [20]; therefore, they are experimentally accessible. An additional selection rule is that $J = 1/2 \rightarrow J' = 1/2$ is forbidden. Such transitions could hypothetically only occur in the case $N = 1 \rightarrow N' = 1$; see also Fig. 3. This case must be treated carefully. We now

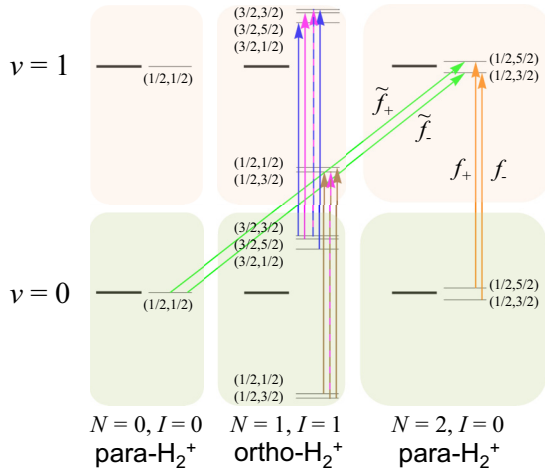


FIG. 3. Schematic of the spin structure of the lowest rovibrational levels of H_2^+ . The number pairs in parentheses are (F, J) . The thick lines represent the spin-averaged energies of the levels. Energy splittings are not to scale. The colored arrows denote transition frequencies to be measured. The weights α are not indicated but are discussed in the text.

discuss the cases of transitions between para states and between ortho states separately.

1. Para- H_2^+

The spin states of para levels ($I = 0$) are simple, pure angular momentum states,

$$N = 0: |N, F = 1/2, J = 1/2\rangle,$$

$$N = 2, 4, \dots: |N, F = 1/2, J = N - 1/2\rangle,$$

$$|N, F = 1/2, J = N + 1/2\rangle.$$

For transitions with $N \rightarrow N' = N$, the traceless frequency is the weighted sum of *two* frequencies (f_- , f_+) corresponding to $\Delta F = 0$, $\Delta J = 0$ transitions, which are shown as orange arrows in Fig. 3:

$$f_t^{\text{spin}} = [(2J_- + 1)f_- + (2J_+ + 1)f_+]/N' = f^{\text{spin-avg}}. \quad (27)$$

Here, $J_{\pm} = N \pm 1/2$. The weights of f_- and f_+ are $N/(2N + 1)$ and $(N + 1)/(2N + 1)$, respectively. The traceless frequency eliminates the effect of the two relevant spin-structure coefficients, $c_e(v, N)$ for the lower level and $c_e(v', N' = N)$ for the upper level.

If one wants to address levels with $N = 0$ one must take into account that transitions with $N = 0 \rightarrow N' = 0$ are forbidden. In this case, the traceless frequency is the weighted sum of *two* transitions with $\Delta N = +2$ (or -2), which start or end at a *common single* state. Now, the two transitions, denoted by \tilde{f}_- , \tilde{f}_+ have $\Delta J = 1$ and $\Delta J = 2$, respectively. We consider the case $N = 0$, $N' = 2$, which is indicated as green arrows in Fig. 3. The spin energy of the $N = 0$ level is zero; therefore,

$$f_t^{\text{spin}} = [(2J'_- + 1)\tilde{f}_- + (2J'_+ + 1)\tilde{f}_+]/N' = f^{\text{spin-avg}}. \quad (28)$$

The weights of \tilde{f}_- and \tilde{f}_+ are $4/10$ and $6/10$, respectively. The traceless frequency eliminates the effect of the single spin

coefficient present in the problem, $c_e(v', N' = 2)$ for the upper level.

2. Ortho- H_2^+

For transitions between ortho levels ($I = 1$) we shall limit ourselves to the case $N \rightarrow N' = N$, which we consider the most experimentally relevant at this time. Thus the spin structure is the same in the initial and final levels. The number of states is $\mathcal{N} = N' = 6(2N + 1)$. The traceless frequency is the weighted sum over all transitions with $\Delta F = 0$, $\Delta J = 0$,

$$\begin{aligned} f_t^{\text{spin}} &= \sum_J [(2J + 1)/\mathcal{N}] f(v, N, F, J \rightarrow v', N, F, J) \\ &= \sum_J [(2J + 1)/\mathcal{N}] (f^{\text{spin-avg}} + E_{v'NFJ}^{\text{spin}} - E_{vNFJ}^{\text{spin}}) \\ &= [6(2N + 1)/\mathcal{N}] f^{\text{spin-avg}} + \sum_J [(2J + 1)/\mathcal{N}] E_{v'NFJ}^{\text{spin}} \\ &\quad - \sum_J [(2J + 1)/\mathcal{N}] E_{vNFJ}^{\text{spin}} \\ &= f^{\text{spin-avg}}(v, N \rightarrow v', N). \end{aligned} \quad (29)$$

The sums include five transitions if $N = 1$ and six transitions if $N = 3, 5, \dots$. The traceless frequency eliminates the effect of 10 spin coefficients, five for the lower level and five for the upper level.

As mentioned, the case $N = 1 \rightarrow N' = 1$ is special because both the initial and the final rovibrational levels include two spin states having total angular momentum $J = 1/2$ and the $\Delta J = 0$ transitions between these are forbidden. Thus two frequencies in the first sum in Eq. (29), $f(N, F = 1/2, J = 1/2 \rightarrow N, F, J' = J)$ and $f(N, F = 3/2, J = 1/2 \rightarrow N, F, J' = J)$, cannot be experimentally accessed. This problem is solved by determining these via a combination of allowed transitions. Several such combinations are possible; one of them is

$$\begin{aligned} &f(N, F = 1/2, J = 1/2 \rightarrow N, F, J' = J) \\ &= f(N, 1/2, 1/2 \rightarrow N, 1/2, 3/2) \\ &\quad - f(N, 1/2, 3/2 \rightarrow N, 1/2, 3/2) \\ &\quad + f(N, 1/2, 3/2 \rightarrow N, 1/2, 1/2). \end{aligned} \quad (30)$$

These three transitions are shown as the two brown arrows and the brown-magenta dashed arrow in the figure. Similarly, $f(N, F = 3/2, J = 1/2 \rightarrow N, F, J' = J)$ can be determined via the transitions shown as the two blue arrows and the blue-magenta dashed arrow in the figure. The remaining three frequencies $f(F = 1/2, J = 3/2 \rightarrow F, J)$, $f(F = 3/2, J = 3/2 \rightarrow F, J)$, and $f(F = 3/2, J = 5/2 \rightarrow F, J)$ are accessible and are shown as the magenta, the magenta-brown dashed, and the magenta-blue dashed arrows in Fig. 3. Because there is a partial overlap in the transitions to be measured, only two additional frequencies are required in order to overcome the $J = 1/2 \not\leftrightarrow J' = 1/2$ selection rule, yielding a total of seven transitions.

All considered transition frequencies have $\Delta F = 0$; thus they lie within a range of approximately 200 MHz for a given rovibrational level, requiring only a single laser for their measurement.

TABLE I. Theoretical [6,20] and experimental spin-structure energies [derived from Eq. (31)] of the $F = 1/2$, $J = 3/2$ spin structure state of ortho- H_2^+ in $N = 1$ rotational states. Values are in MHz.

v	Theoretical	Experimental
4	-842.4234	-842.4230
5	-824.5255	-824.5253
6	-808.0888	-808.0888
7	-793.0463	-793.0464
8	-779.3412	-779.3418

3. Application to the results of Jefferts (1969)

Jefferts [21] measured with high resolution radiofrequency (rf) transitions of H_2^+ , both in the para levels $N = 2$, $v = 4, 5, 6, 7, 8$, and in the ortho levels $N = 1$, $v = 4, 5, 6, 7, 8$.

In the $N = 2$ levels there is but a single frequency, corresponding to the transition $F = 1/2$, $J = 3/2 \rightarrow F' = F$, $J' = 5/2$ (see Fig. 3). Due to the simplicity of the spin Hamiltonian in this case, both spin energies are given by the rf frequency multiplied by a known coefficient [19].

The rf transition frequencies obtained for the $N = 1$ states can be combined with the tracelessness condition of the spin Hamiltonian to provide additional information, the actual spin-structure energies $E_{p,m}^{\text{spin}}$. Let us denote the five rf transition frequencies measured by Jefferts in each vibrational level (columns 2–6 of his Table I) by $f_{v,1}$, $f_{v,2}$, $f_{v,3}$, $f_{v,4}$, $f_{v,5}$. Of these, only four are independent. The tracelessness condition yields

$$E_{v,1,F=\frac{1}{2},J=\frac{3}{2}}^{\text{spin}} = -\frac{1}{9}(-f_{v,2} + f_{v,3} + 3f_{v,4} + 3f_{v,5}). \quad (31)$$

From this particular value, the spin energies of the other spin states can be trivially obtained. As a further step, the spin energies of different vibrational levels can be subtracted to yield the spin-structure contributions $f^{\text{spin}}(v, 1, F, J \rightarrow v', 1, F', J')$. Thus, the combination of rf spectroscopy for both the lower and upper rovibrational level and a single rovibrational spin component measured by laser spectroscopy can also furnish the spin-averaged rovibrational frequency.

In Table I we compare the values of the spin energies derived from Jefferts' data with the most precise *ab initio* values recently obtained [20] on the basis of the theory of Ref. [6]. Jefferts assigned an uncertainty of 1.5 kHz to each transition frequency value $f_{v,i}$, which he related to inhomogeneous Zeeman shifts. If we assume Gaussian statistics, the experimental error of $E_{v,1,F=\frac{1}{2},J=\frac{3}{2}}^{\text{spin}}$ then is $0.5 \times (1.5 \text{ kHz})$. The table shows that this experimental error is consistent with the deviations between theoretical and experimental values.

VII. CANCELING THE SYSTEMATIC SHIFTS

A. Partial cancellation

Line 1 in Table II summarizes the discussion of Sec. VI, the case of traceless frequency where the Zeeman components and thus the systematic shifts are not considered. Line 2 is the case where the LZ shift is canceled, but all other shifts are not canceled, except in particular cases. We denote this traceless frequency by $f_t^{\text{spin,LZ}}$. It will be discussed next.

I. H_2^+

Cancellation of the LZ shift in the traceless frequency is implemented, for H_2^+ , by measuring, for each $J \rightarrow J'$ transition, the pair $J_z \rightarrow J'_z$, $-J_z \rightarrow -J'_z$. The values of J_z , J'_z can be chosen freely. Thus there is a substantial number of options for implementation. This requires doubling the number of spin components to be measured, compared to the case of line 1. For transitions between the para states of H_2^+ shown in Fig. 3 (green or orange arrows), the number is four, still small. For such transitions, the resulting EQ, Stark, and QZ shifts are reported in Table III. The table shows all six possible options for the $(0, 0) \rightarrow (1, 2)$ transition and a subset of all options for the $(0, 2) \rightarrow (1, 2)$ transition.

The EQ shift in para states of H_2^+ was computed using

$$E^{\text{EQ}}(v, N, F, S, J, J_z) = \frac{3}{2} \sqrt{\frac{3}{2}} E_{14}(v, N) \times \left(-\frac{1}{2} \frac{D'[J(J+1) - 3J_z^2]}{3J(J+1)(2J-1)(2J+3)} \right) V_{zz},$$

where $D' = 3D(D-1) - 4J(J+1)N(N+1)$ and $D = J(J+1) + N(N+1) - 3/4$. This results from Eq. (40) in [11] and Eqs. (10) and (25) in [12]. $E_{14}(v, N)$ is the quadrupole coupling coefficient.

In the table, we recognize two cases in which the QZ shift is zero (underlined). Clearly, these are the transitions of choice. For an electric-field gradient assumed to be $V_{zz} \simeq 0.07 \text{ GV/m}^2$, the shift of these two transitions is 5 Hz ($\simeq 1 \times 10^{-13}$) and -0.6 Hz ($\simeq 1 \times 10^{-14}$), respectively.

For the first transition, $(0, 0) \rightarrow (1, 2)$, the LZ shifts of the contributing Zeeman transitions, weighted according to Eq. (28), are $\simeq -56 \text{ kHz/G}$ and $\simeq 252 \text{ kHz/G}$, respectively. This means that in a magnetic field $B = 0.1 \text{ G}$, its stability must be better than 1 part in 5000, if the residual LZ after averaging over the Zeeman components is to be smaller than the EQ shift.

For the second transition, $(0, 2) \rightarrow (1, 2)$, the weighted LZ shifts are approximately 10^5 times smaller, $\simeq 0.9 \text{ Hz/G}$ and $\simeq 2.5 \text{ Hz/G}$, respectively. Thus no high magnetic field stability is needed. This is an attractive choice for high-precision measurements.

The order of magnitude for the time-averaged electric field squared in a macroscopic linear ion trap is $E^2 \simeq 1 \text{ (kV/m)}^2$, whereupon the dc Stark shift is approximately 10 mHz for all transitions shown in the table, or $\leq 2 \times 10^{-16}$ fractionally.

With the options given by Table III it is easy to consider the combination of two transitions, $f_c = \beta_1 f_{t,1}^{\text{spin,LZ}} + \beta_2 f_{t,2}^{\text{spin,LZ}}$, with the weights satisfying the condition $\beta_1 + \beta_2 = 1$ in order not to suppress the spin-averaged frequency. A total of eight Zeeman components would need to be measured. Particularly attractive is the combination of the last two transitions in the table. They can be combined either to null the composite EQ shift, resulting in a composite QZ shift of 0.0028 kHz/G^2 , or to null the composite QZ shift, giving a composite EQ shift of $0.091 \text{ Hz m}^2/\text{GV}$. In practice, the nulling can only be as good as the stability of the fields during measurement. It may then be more robust to combine the 11th and 12th transitions (bold in the table), which have smaller shifts. The individual Zeeman components contribute with very small LZ shifts of $\simeq 4 \text{ Hz/G}$ or less, so that magnetic-field stability is not an

TABLE II. Overview of the number n of Zeeman components to be measured in order to achieve traceless frequencies with different cancellation of systematic shifts. The expressions in parentheses denote the contributing transitions $J \rightarrow J'$. The asterisk (*) indicates that there exist particular choices that in addition have zero QZS. The double asterisks (**) indicate cases where more efficient strategies can achieve lower number of transitions to be measured; see Sec. VIII. SS: spin structure; LZS: linear Zeeman shift; QZS: quadratic Zeeman shift; EQS: electric quadrupole shift.

Cancellation of	$H_2^+ (E2)$		$HD^+ (E1)$
	$N = 0 \rightarrow N' = 2$	$N = 2 \rightarrow N' = 2$	$N = 0 \rightarrow N' = 1$
(1) SS (f_t^{spin})	$1(\frac{1}{2} \rightarrow \frac{3}{2}) + 1(\frac{1}{2} \rightarrow \frac{5}{2}) = 2$	$1(\frac{3}{2} \rightarrow \frac{3}{2}) + 1(\frac{5}{2} \rightarrow \frac{5}{2}) = 2$	10 (Fig. 2)
(2) SS, LZS ($f_t^{\text{spin,LZ}}$)	$2(\frac{1}{2} \rightarrow \frac{3}{2}) + 2(\frac{1}{2} \rightarrow \frac{5}{2}) = 4 *$	$2(\frac{3}{2} \rightarrow \frac{3}{2}) + 2(\frac{5}{2} \rightarrow \frac{5}{2}) = 4 *$	10 (Fig. 2)
(3) SS, LZS, QZS, EQS ($f_t^{\text{pert-free}}$)	$4(\frac{1}{2} \rightarrow \frac{3}{2})$ $+6(\frac{1}{2} \rightarrow \frac{5}{2}) = 10 **$	$4(\frac{3}{2} \rightarrow \frac{3}{2})$ $+6(\frac{5}{2} \rightarrow \frac{5}{2}) = 10 **$	$9 + 5 + 15(2 \rightarrow 1, 2, 3) + 3 + 3$ $+9(1 \rightarrow 0, 1, 2) + 3(0 \rightarrow 1)$ $+3 + 3 + 9(1 \rightarrow 0, 1, 2) = 62 **$

issue. If the combination is chosen to null the QZ shift, the remaining dominant shift is the EQ shift. For the field strength value assumed above, we may expect a fractional shift of approximately 2×10^{-15} .

Note that such combinations f_c contain only one transition pair less than the general expression, i.e., 8 vs 10 Zeeman components. Even more efficient combinations will be presented below in Sec. VIII.

The smallness of the LZ shift and QZ shift of the individual Zeeman components entering the second zero-QZ shift transition (underlined in the table) and the 11th and 12th transitions was already emphasized earlier by us [9].

2. HD^+

For cancellation of LZ shift in HD^+ , we can choose to measure only the particular components $J_z = 0 \rightarrow J'_z = 0$, and the number of spin components to be measured remains the same as in line 1. Table IV includes transitions with different (N, N') , and shows several $E1$ transitions. The EQ shift was computed following Ref. [11]. For the electric-field gradient $V_{zz} \simeq 0.07 \text{ GV/m}^2$ and a typical magnetic field $B \simeq 0.1 \text{ G}$, the two $E1$ vibrational transitions, $(0, 0) \rightarrow (1, 1)$, $(0, 1) \rightarrow (1, 2)$, have a shift of approximately 150 Hz, or 2×10^{-12} , dominated by QZ shifts. These absolute values are also the case for the two pure rotational transitions. But since these

TABLE III. H_2^+ : the contributions of systematic shifts to traceless frequencies $f_t^{\text{spin,LZ}}$ which include only one pair of Zeeman components per hyperfine transition. The spin-structure contributions cancel and the linear Zeeman shift is zero for all cases. For each rovibrational transition, the cases are ordered according to an increasing absolute value of the EQ shift. For the $(0, 2) \rightarrow (1, 2)$ transition, the first 11 and the last 2 of the 36 possible cases are shown. n is the number of transitions that contribute to $f_t^{\text{spin,LZ}}$. The third column reports (omitting the signs) the values $\pm J_z \rightarrow \pm J'_z$ of the $J = 1/2 \rightarrow J' = 3/2$, $J = 1/2 \rightarrow J' = 5/2$ hyperfine transitions (in the upper section) or of the $J = 3/2 \rightarrow J' = 3/2$, $J = 5/2 \rightarrow J' = 5/2$ transitions (in the lower section). θ is the angle between the electric-field vector and the magnetic-field vector (quantization axis).

Transition	n	Zeeman components	EQ shift/ V_{zz} (Hz m^2/GV)	dc Stark shift/ E^2 (Hz $(\text{m/kV})^2$)	QZ shift/ B^2 (kHz/ G^2)
$E2 : (0, 0) \rightarrow (1, 2)$	4	$\frac{1}{2} \rightarrow \frac{3}{2}, \frac{1}{2} \rightarrow \frac{3}{2}$	29.2	$0.0033 \cos^2 \theta - 0.011$	2.54
$E2 : (0, 0) \rightarrow (1, 2)$	4	$\frac{1}{2} \rightarrow \frac{3}{2}, \frac{1}{2} \rightarrow \frac{1}{2}$	-36.4	$-0.0041 \cos^2 \theta - 0.0082$	6.35
$E2 : (0, 0) \rightarrow (1, 2)$	4	$\frac{1}{2} \rightarrow \frac{1}{2}, \frac{1}{2} \rightarrow \frac{5}{2}$	58.3	$0.0066 \cos^2 \theta - 0.012$	-7.63
<u>$E2 : (0, 0) \rightarrow (1, 2)$</u>	4	<u>$\frac{1}{2} \rightarrow \frac{1}{2}, \frac{1}{2} \rightarrow \frac{3}{2}$</u>	-72.9	$-0.0082 \cos^2 \theta - 0.0068$	0
$E2 : (0, 0) \rightarrow (1, 2)$	4	$\frac{1}{2} \rightarrow \frac{1}{2}, \frac{1}{2} \rightarrow \frac{1}{2}$	-139	$-0.016 \cos^2 \theta - 0.0043$	3.81
$E2 : (0, 0) \rightarrow (1, 2)$	4	$\frac{1}{2} \rightarrow \frac{3}{2}, \frac{1}{2} \rightarrow \frac{5}{2}$	160	$0.018 \cos^2 \theta - 0.016$	-5.08
$E2 : (0, 2) \rightarrow (1, 2)$	4	$\frac{3}{2} \rightarrow \frac{3}{2}, \frac{3}{2} \rightarrow \frac{3}{2}$	3.63	$0.00098 \cos^2 \theta - 0.0095$	0.156
$E2 : (0, 2) \rightarrow (1, 2)$	4	$\frac{3}{2} \rightarrow \frac{3}{2}, \frac{1}{2} \rightarrow \frac{1}{2}$	-4.53	$-0.0012 \cos^2 \theta - 0.0088$	0.390
$E2 : (0, 2) \rightarrow (1, 2)$	4	$\frac{1}{2} \rightarrow \frac{1}{2}, \frac{5}{2} \rightarrow \frac{5}{2}$	7.25	$0.0020 \cos^2 \theta - 0.0098$	-0.469
$E2 : (0, 2) \rightarrow (1, 2)$	4	$\frac{1}{2} \rightarrow \frac{1}{2}, \frac{3}{2} \rightarrow \frac{3}{2}$	-9.07	$-0.0024 \cos^2 \theta - 0.0084$	0
$E2 : (0, 2) \rightarrow (1, 2)$	4	$\frac{1}{2} \rightarrow \frac{1}{2}, \frac{1}{2} \rightarrow \frac{1}{2}$	-17.2	$-0.0046 \cos^2 \theta - 0.0076$	0.234
$E2 : (0, 2) \rightarrow (1, 2)$	4	$\frac{1}{2} \rightarrow \frac{3}{2}, \frac{1}{2} \rightarrow \frac{3}{2}$	19.9	$0.0054 \cos^2 \theta - 0.011$	-0.312
$E2 : (0, 2) \rightarrow (1, 2)$	4	$\frac{1}{2} \rightarrow \frac{3}{2}, \frac{1}{2} \rightarrow \frac{5}{2}$	-21.9	$-0.0013 \cos^2 \theta - 0.0087$	9.70
$E2 : (0, 2) \rightarrow (1, 2)$	4	$\frac{1}{2} \rightarrow \frac{3}{2}, \frac{1}{2} \rightarrow \frac{1}{2}$	27.4	$0.0017 \cos^2 \theta - 0.0097$	6.35
$E2 : (0, 2) \rightarrow (1, 2)$	4	$\frac{1}{2} \rightarrow \frac{1}{2}, \frac{3}{2} \rightarrow \frac{3}{2}$	32.8	$0.0043 \cos^2 \theta - 0.011$	-10.0
$E2 : (0, 2) \rightarrow (1, 2)$	4	$\frac{1}{2} \rightarrow \frac{1}{2}, \frac{1}{2} \rightarrow \frac{5}{2}$	-41.0	$-0.0053 \cos^2 \theta - 0.0074$	-5.96
$E2 : (0, 2) \rightarrow (1, 2)$	4	$\frac{1}{2} \rightarrow \frac{1}{2}, \frac{1}{2} \rightarrow \frac{3}{2}$	48.4	$0.0027 \cos^2 \theta - 0.010$	-3.58
$E2 : (0, 2) \rightarrow (1, 2)$	4	$\frac{1}{2} \rightarrow \frac{1}{2}, \frac{5}{2} \rightarrow \frac{5}{2}$	-279	$-0.028 \cos^2 \theta + 0.00025$	8.58
$E2 : (0, 2) \rightarrow (1, 2)$	4	$\frac{1}{2} \rightarrow \frac{3}{2}, \frac{1}{2} \rightarrow \frac{5}{2}$	282	$0.029 \cos^2 \theta - 0.019$	-8.66

TABLE IV. HD⁺: examples of the contributions of systematic shifts to traceless frequencies $f_t^{\text{spin,LZ}}$, which include only the $J_z = 0 \rightarrow J'_z = 0$ components for each hyperfine transition, according to Eq. (20). The spin-structure contributions cancel and the linear Zeeman shift is zero for all cases.

Transition	n	EQ shift/ V_{zz} (Hz m ² /GV)	dc Stark shift/ E^2 (Hz (m/kV) ²)	QZ shift/ B^2 (kHz/G ²)
$E1 : (0, 0) \rightarrow (0, 1)$	10	-37	$4.6 + 0.68 \cos^2 \theta$	-14
$E1 : (0, 1) \rightarrow (0, 2)$	22	-48	$0.054 - 0.16 \cos^2 \theta$	15
$E1 : (0, 0) \rightarrow (1, 1)$	10	-41	$4.6 + 0.79 \cos^2 \theta$	-15
$E1 : (0, 1) \rightarrow (1, 2)$	22	-59	$0.016 - 0.076 \cos^2 \theta$	15
$E2 : (0, 0) \rightarrow (1, 2)$	12	-95	$4.7 + 0.60 \cos^2 \theta$	1.4
$E2 : (0, 1) \rightarrow (1, 1)$	10	-4.6	$-0.047 + 0.12 \cos^2 \theta$	-0.75
$E2 : (0, 2) \rightarrow (1, 2)$	12	-11	$-0.038 + 0.087 \cos^2 \theta$	0.27
$E2 : (0, 2) \rightarrow (1, 0)$	12	85	$-5.5 - 0.52 \cos^2 \theta$	-1.0

have $\simeq 45$ or 15 times smaller frequency, the fractional shifts are $\simeq (1, 0.3) \times 10^{-10}$, respectively.

Table IV also includes electric quadrupole transitions ($E2$). It is unusual to consider such transitions for heteronuclear diatomic molecules, but we see from the table that for a given lower rovibrational level they reduce significantly the number of Zeeman components to be measured. In addition, for the vibrational transitions with $\Delta J = \pm 2$ the QZ shifts are reduced by a factor of approximately 10 compared to the $E1$ transitions. The total shift is of order 10 Hz (2×10^{-13} fractionally), still dominated by the QZ shift. For the $\Delta J = 0$ transitions, the QZ shift is even smaller, e.g., for the $(0, 2) \rightarrow (1, 2)$ transition, the total shift is $\simeq 3$ Hz, or 5×10^{-14} . This is an attractive transition for high-precision experiments.

B. Largely complete cancellation: General method

According to the general formula Eq. (20) we can combine the spin-structure cancellation (which did not consider the individual Zeeman components $J_z \rightarrow J'_z$) with a cancellation of the Zeeman and EQ shifts. This will typically require one to increase substantially the number of Zeeman components to be measured. Table II, case (3), indicates this number. It is obtained directly from Fig. 1.

An example will illustrate the cancellation of the quadratic Zeeman shift. Consider HD⁺ and the transition shown in Fig. 2. The double sum over m, m' in Eq. (17) includes all J_z and all J'_z . Consider the contributions having a particular value of J'_z or of J_z . With the help of Figs. 1(a)–1(c) we find the weights $\tilde{\alpha}$ in the traceless frequency $f_t^{\text{pert-free}}$, to be assigned to the transitions

TABLE V. Explanation of cancellation of QZ shift in $f_t^{\text{pert-free}}$. Upper table: weights $\tilde{\alpha}$ for the frequencies of the transitions connecting to the $J'_z = -1$ states of the $N' = 1$ rovibrational level in a $N = 0 \rightarrow N' = 1$ transition. The first factor in each entry is, from Fig. 2, $(2J' + 1)/N'$, where $N' = \sum_{m'} = 36$. The second factor is obtained from Fig. 1, with the panel letter indicated in the entry. It contains the sum of the weights of those Zeeman components J_z of the given lower level FSJ that connect to J'_z . The product of the two factors is $1/[(2|J'_z| + 1)N']$, and thus each entry is equal for all the considered states. These equal values enter f_t and allow nulling the QZ shift according to Eq. (17). Lower table: same as (a), but for the $J_z = 0$ states of the $N = 0$ level of the same transition. The sum of weights of the transitions reaching a particular $FSJ, J_z = 0$ is shown in the last column. Those values being all equal allows one to null the QZ shift in f_t , according to Eq. (17).

Lower level FSJ		Upper level			
$F'S'$		J'			
		0	1	2	3
122	12	(b): $(3/36) \times (\frac{3}{15} + \frac{1}{15} + \frac{1}{15})$		$(5/36) \times (\frac{1}{5})$	(c): $(7/36) \times (\frac{1}{35} + \frac{1}{35} + \frac{3}{35})$
111	11	(a): $(3/36) \times (\frac{1}{3})$		(b): $(5/36) \times (\frac{1}{15} + \frac{2}{15})$	
100	10	(a): $(3/36) \times (\frac{1}{3})$			
011	01	(a): $(3/36) \times (\frac{1}{3})$		(b): $(5/36) \times (\frac{1}{15} + \frac{2}{15})$	

Lower level	Upper level				$\sum_{m'} \tilde{\alpha}(p', m'; p, m)$	
FSJ	$F'S'$	J'				
		0	1	2	3	
122	12		(b): $(3/36) \times (\frac{1}{15} + \frac{1}{15} + \frac{1}{15})$	$(5/36) \times (\frac{1}{5})$	(c): $(7/36) \times (\frac{3}{35} + \frac{1}{35} + \frac{3}{35})$	3/36
111	11	(a): $(1/36) \times (\frac{1}{3})$	(a): $(3/36) \times (\frac{1}{3})$	(b): $(5/36) \times (\frac{2}{15} + \frac{1}{15} + \frac{2}{15})$		3/36
100	10		(a): $(3/36) \times 1$			3/36
011	01	(a): $(1/36) \times (\frac{1}{3})$	(a): $(3/36) \times (\frac{1}{3})$	(b): $(5/36) \times (\frac{2}{15} + \frac{1}{15} + \frac{2}{15})$		3/36

TABLE VI. H_2^+ : Contributions of residual systematic shifts to traceless frequencies $f_t^{\text{pert-free}}$, which are sums over all Zeeman components, according to Eq. (20). For all cases, the spin-structure contributions cancel and the linear Zeeman shift, the quadratic shift, and the electric quadrupole shifts average to zero.

Transition	n	dc Stark shift/ E^2 (Hz (m/kV) 2)
$H_2^+ : E2, (0, 0) \rightarrow (1, 2)$	10	-0.0048
$H_2^+ : E2, (0, 2) \rightarrow (1, 2)$	10	-0.0046
$HD^+ : E1, (0, 0) \rightarrow (0, 1)$	62	4.9
$HD^+ : E1, (0, 1) \rightarrow (0, 2)$	142	-0.00024
$HD^+ : E1, (0, 0) \rightarrow (1, 1)$	62	4.9
$HD^+ : E1, (0, 1) \rightarrow (1, 2)$	142	-0.0092
$HD^+ : E1, (0, 0) \rightarrow (1, 2)$	104	4.9
$HD^+ : E2, (0, 1) \rightarrow (1, 1)$	36	-0.0089
$HD^+ : E2, (0, 2) \rightarrow (1, 2)$	60	-0.0089

connecting to the different $F S J, F' S' J'$ states. Table V shows two cases, $J'_z = -1$ and $J_z = 0$. It is seen that the QZ shift stemming from all transitions to each of these states is indeed nulled.

The same results hold also for the contributions arising from the other J'_z and J_z states. Thus $f_t^{\text{pert-free}}$ is free of QZ shift.

The EQ shift is canceled in the summation over all J_z and J'_z . This also cancels the tensor Stark shift, but not the scalar Stark shift. It affects all spin states of a given rovibrational level equally. It is nonzero for all values N and is v -, N -dependent [12].

Table VI gives the values of the Stark shifts for H_2^+ and HD^+ , respectively. The values will not vary much for different choices of the vibrational levels v, v' .

For H_2^+ , the residual shifts are negligible, below 1×10^{-16} .

For transitions of HD^+ involving $N = 0$ levels, due to their large scalar polarizability, the Stark shifts are not negligible. Assuming as before $E^2 \simeq 1$ (kV/m) 2 , the shift for the fundamental rotational and the fundamental vibrational transition is approximately 4×10^{-12} and 1×10^{-13} , respectively. We see again the advantage of $E2$ transitions: the transition $(0, 1) \rightarrow$

$(1, 1)$ has a negligible shift and also the smallest number of transitions (36) among the shown set. This number is, unfortunately, still rather large.

VIII. LARGELY COMPLETE CANCELLATION: OPTIMIZED METHOD

Especially for the case of HD^+ , the number of transitions for achieving cancellation of systematics in $f_t^{\text{pert-free}}$ is large. In this section we present more efficient solutions for traceless frequencies, f_t^{opt} , that have zero LZ, QZ, and EQ shifts, for both H_2^+ and HD^+ .

A. H_2^+

For the $(0, 0) \rightarrow (1, 2)$ transition, among the Zeeman components we select those five having the smallest LZ shifts. They are marked with red disks and arrows in Figs. 1(d) and 1(e). We make the ansatz

$$f_t^{\text{opt}}(0, 0 \rightarrow 1, 2) = \frac{4}{10} \left[\alpha \tilde{f}_- \left(J_z = \frac{1}{2} \rightarrow J'_z = -\frac{1}{2} \right) + (1 - \alpha) \tilde{f}_- \left(\frac{1}{2} \rightarrow -\frac{3}{2} \right) \right] + \frac{6}{10} \left[\beta \tilde{f}_+ \left(\frac{1}{2} \rightarrow \frac{1}{2} \right) + \gamma \tilde{f}_+ \left(\frac{1}{2} \rightarrow \frac{3}{2} \right) + (1 - \beta - \gamma) \tilde{f}_+ \left(\frac{1}{2} \rightarrow \frac{5}{2} \right) \right]. \quad (32)$$

The transitions \tilde{f}_-, \tilde{f}_+ are indicated in Fig. 3. The spin-structure contributions cancel for any value of the weights α, β, γ . They are determined by imposing the vanishing of the LZ shift, the QZ shift, and the EQ shift. The result is shown in Table VII. As mentioned above, except for the $\tilde{f}_+(\frac{1}{2} \rightarrow \frac{5}{2})$ transition, the LZ shifts of the individual Zeeman components in f_t^{opt} are rather large, the largest being 2.5 MHz/G. Therefore, the stability of the magnetic field during the course of the measurement of the complete set of transitions is a serious issue if ultrahigh accuracy (Hz level) is aimed for. The table also shows the largest QZ shift, which in comparison is not important.

TABLE VII. The contributions of residual systematic shifts to traceless frequencies f_t^{opt} which are produced from a minimized number n of Zeeman components. For all cases, the spin-structure contributions cancel, and the LZ shift, QZ shift, and EQ shift average to zero. The weights in column 3 are (α, β, γ) for H_2^+ and (α, β) for HD^+ . The numerical values are rounded. The last two columns list the largest individual effective QZ shift (QZS) and effective LZ shift (LZS) among all Zeeman components i contributing to f_t^{opt} . Effective here means that the QZS_i and LZS_i are corrected for the weight with which the component i contributes.

Transition	n	Weights	dc Stark shift/ E^2 (Hz (m/kV) 2)	Max(QZS $_i$)/ B^2 (kHz/G 2)	Max(LZS $_i$)/ B (kHz/G)
$H_2^+ : E2, (0, 0) \rightarrow (1, 2)$	5	$(\frac{1}{2}, -\frac{11}{3}, \frac{19}{3})$	-0.0095	48	2470
$H_2^+ : E2, (0, 2) \rightarrow (1, 2)$	5	$(\frac{1}{2}, \frac{16}{3}, -\frac{43}{6})$	-0.0092	3.7	0.037
$H_2^+ : E2, (0, 1) \rightarrow (1, 1)$	10	$(1.67, 2.40, 3.45 \times 10^3)$	-0.0091	3.5	23
$HD^+ : E1, (0, 0) \rightarrow (0, 1)$	14	$(0.337, 0.715)$	4.9	21	0.79
$HD^+ : E1, (0, 0) \rightarrow (1, 1)$	14	$(-0.362, 0.684)$	4.9	23	0.85
$HD^+ : E2 : (0, 0) \rightarrow (1, 2)$	16	$(0.792, -7.53)$	4.9	5.1	5.8
$HD^+ : E2, (0, 1) \rightarrow (1, 1)$	14	$(5.47, 1.002)$	$-0.0089 + 3 \times 10^{-5} \cos^2 \theta$	8.0	0.087
$HD^+ : E2, (0, 2) \rightarrow (1, 2)$	16	$(26.3, 3.59)$	$-0.025 + 0.049 \cos^2 \theta$	2.6	1.9
$HD^+ : E2, (0, 2) \rightarrow (1, 0)$	16	$(0.677, -1.80)$	-5.7	4.1	5.4

For the $(0, 2) \rightarrow (1, 2)$ transition, among the Zeeman components, those having $J_z \rightarrow J'_z = J_z$ exhibit very small LZ shifts (<15 Hz/G) and small QZ shifts (<1.2 kHz/G²). We choose them for the ansatz

$$\begin{aligned} f_t^{\text{opt}}(0, 2 \rightarrow 1, 2) = & \frac{4}{10} \left[\alpha f_- \left(J_z = \frac{1}{2} \rightarrow J'_z = \frac{1}{2} \right) \right. \\ & \left. + (1 - \alpha) f_- \left(\frac{3}{2} \rightarrow \frac{3}{2} \right) \right] \\ & + \frac{6}{10} \left[\beta f_+ \left(\frac{1}{2} \rightarrow \frac{1}{2} \right) + \gamma f_+ \left(\frac{3}{2} \rightarrow \frac{3}{2} \right) \right] \\ & + (1 - \beta - \gamma) f_+ \left(\frac{5}{2} \rightarrow \frac{5}{2} \right). \quad (33) \end{aligned}$$

The transitions f_- , f_+ are indicated in Fig. 3. The result of the external-field shift cancellation is reported in Table VII. Transition (33) is especially attractive, since the residual shift is negligible. Note that the effect of two spin-structure coefficients and three systematic shifts are canceled with only five transitions.

The $(0, 1) \rightarrow (1, 1)$ transition requires more components. The ansatz uses the traceless frequency f_t^{spin} of Eqs. (29) and (30) (with a particular choice of Zeeman components), leading to a LZ shift of 16.4 kHz/G, a QZ shift of 0.493 kHz/G², and an EQ shift of 1.76 Hz/(GV/m²), and adds additional contributions that allow one to null LZ, QZ, and EQ shifts:

$$\begin{aligned} f_t^{\text{opt}}(0, 1 \rightarrow 1, 1) = & f_t^{\text{spin}} + \frac{4\alpha}{18} \left[f \left(\frac{1}{2}, \frac{3}{2}, \frac{3}{2} \rightarrow \frac{1}{2}, \frac{3}{2}, \frac{3}{2} \right) \right. \\ & \left. - f \left(\frac{1}{2}, \frac{3}{2}, \frac{1}{2} \rightarrow \frac{1}{2}, \frac{3}{2}, \frac{1}{2} \right) \right] \\ & + \frac{4\beta}{18} \left[f \left(\frac{3}{2}, \frac{3}{2}, \frac{3}{2} \rightarrow \frac{3}{2}, \frac{3}{2}, \frac{3}{2} \right) \right. \\ & \left. - f \left(\frac{3}{2}, \frac{3}{2}, \frac{1}{2} \rightarrow \frac{3}{2}, \frac{3}{2}, \frac{1}{2} \right) \right] \\ & + \frac{6\gamma}{18} \left[f \left(\frac{3}{2}, \frac{3}{2}, -\frac{5}{2} \rightarrow \frac{3}{2}, \frac{3}{2}, -\frac{5}{2} \right) \right. \\ & \left. - f \left(\frac{3}{2}, \frac{5}{2}, \frac{5}{2} \rightarrow \frac{3}{2}, \frac{5}{2}, \frac{5}{2} \right) \right]. \quad (34) \end{aligned}$$

The numbers in parentheses are $F, J, J_z \rightarrow F', J', J'_z$. The resulting solution (see Table VII) exhibits a large γ because of the relatively small LZ shifts of the two frequencies in the last square parenthesis as compared to the other. The largest individual LZ shift is of moderate magnitude, so this is a viable solution as well. The number of different Zeeman components is 10 (seven being included in f_t^{spin} , see Sec. VIC2, and the square parentheses actually containing only three additional ones). With this number, the effect of $5 + 5 = 10$ spin-structure coefficients and of three systematic shifts is nulled. Note that the ansatz above is not unique and is possibly not the most favorable in terms of minimization of the individual components' shifts.

B. HD⁺

For this molecule we construct efficient solutions in a fashion similar to Eq. (34). The main contribution is the traceless frequency $f_t^{\text{spin,LZ}}$ composed of $J_z = 0 \rightarrow J'_z = 0$ transitions, so that the LZ shift is already zero. We add two pairs of Zeeman components of two different hyperfine transitions M_1, M_2 . Being pairs, they do not generate a LZ shift. They allow one to null the overall QZ shift and EQ shift, if their weights are properly chosen.

As a first example, we consider the $(0, 0) \rightarrow (1, 1)$ transition. We choose $M_1 : F S J = 122 \rightarrow F' S' J' = 123$ and $M_2 : F S J = 011 \rightarrow F' S' J' = 012$. The ansatz reads

$$\begin{aligned} f_t^{\text{opt}}(0, 0 \rightarrow 1, 1) = & f_t^{\text{spin,LZ}} + \frac{7}{36} \left[(\alpha - 1) f_{M_1}(J_z = 0 \rightarrow J'_z = 0) \right. \\ & \left. + \frac{1 - \alpha}{2} [f_{M_1}(2 \rightarrow 3) + f_{M_1}(-2 \rightarrow -3)] \right] \\ & + \frac{5}{36} \left[(\beta - 1) f_{M_2}(0 \rightarrow 0) \right. \\ & \left. + \frac{1 - \beta}{2} [f_{M_2}(1 \rightarrow 2) + f_{M_2}(-1 \rightarrow -2)] \right]. \quad (35) \end{aligned}$$

Here, $f_t^{\text{spin,LZ}}$ is the frequency from Table IV. Note that in each square parenthesis the spin and the LZ contributions cancel. The individual LZ shifts of the chosen Zeeman components f_{M_1}, f_{M_2} are ± 0.6 kHz/G and ± 38 kHz/G, respectively. The result of the cancellation is reported in Table VII. We see that the total weights of the individual components significantly reduce their LZ shifts to small and tolerable values. As discussed, the scalar Stark shift is substantial for this particular rovibrational transition, here of order 1×10^{-13} .

A similar procedure can be applied to other rovibrational transitions, both $E1$ and $E2$. The number of Zeeman components increases by four in every case.

For the $E2$ transition $(0, 1) \rightarrow (1, 1)$, we choose, for example, $M_1 : F S J = 122 \rightarrow F' S' J' = 122$ and $M_2 : F S J = 011 \rightarrow F' S' J' = 011$. The ansatz reads

$$\begin{aligned} f_t^{\text{opt}}(0, 1 \rightarrow 1, 1) = & f_t^{\text{spin,LZ}} + \frac{5}{36} \left[(\alpha - 1) f_{M_1}(J_z = 0 \rightarrow J'_z = 0) \right. \\ & \left. + \frac{1 - \alpha}{2} [f_{M_1}(1 \rightarrow 1) + f_{M_1}(-1 \rightarrow -1)] \right] \\ & + \frac{3}{36} \left[(\beta - 1) f_{M_2}(0 \rightarrow 0) \right. \\ & \left. + \frac{1 - \beta}{2} [f_{M_2}(1 \rightarrow 1) + f_{M_2}(-1 \rightarrow -1)] \right]. \quad (36) \end{aligned}$$

The solution, shown in Table VII, indicates that the scalar Stark shift is reduced by approximately a factor 500, to the 2×10^{-16} level. The closeness of β to the value 1 indicates that the inclusion of only the M_1 pair of transitions already leads to a small EQ shift [-1.3 Hz/(GV/m²)]. A second advantage is that the LZ shifts of the individual contributions in Eq. (36)

are at most ± 0.09 kHz/G, so that magnetic-field stability is substantially less demanding than for the $E1$ transition.

An additional four rovibrational transitions are shown in the table. We can state that all HD^+ transitions shown are attractive, with the two $E2$ transitions having $\Delta N = 0$ being particularly attractive, due to their negligible dc Stark shift.

C. Note

Karr *et al.* [8] proposed the following composite frequency for nulling of LZ, QZ, and EQ shifts of the $(v = 0, N = 0) \rightarrow (v' = 2, N' = 2)$ transition of H_2^+ ,

$$\begin{aligned} f_c^{\text{pert-freee}} = & [3 \tilde{f}_+(J_z = \pm 1/2 \rightarrow J'_z = \pm 5/2) \\ & + 2 \tilde{f}_+(\pm 1/2 \rightarrow \pm 1/2) \\ & + 2 \tilde{f}_-(\pm 1/2 \rightarrow \pm 1/2)]/7. \end{aligned} \quad (37)$$

A shorthand notation has been used to indicate the average of a Zeeman component pair. These six Zeeman components are marked with brown disks in Figs. 1(d) and 1(e). The number is smaller by four (two pairs) compared to the general approach but larger by one compared to the optimized method. Cancellation of the spin-structure contributions was not imposed. Indeed, $f_c^{\text{pert-freee}} = f^{\text{spin-avg}} + \{10(N'c'_e/2) + 4[-(N' + 1)c'_e/2]\}/14 = f^{\text{spin-avg}} + 2c'_e/7$.

IX. DISCUSSION AND CONCLUSIONS

We have discussed approaches to null the effect of the perturbation energy shifts arising in the lower and upper levels of quantum systems by considering composite transition frequencies. A fundamental property of certain Hamiltonians, the tracelessness, and the structure of the perturbation expressions must be used as guiding principles for identifying a set of contributing transition frequencies and their corresponding weights. It is remarkable that the number of transitions required to cancel the effect of the spin Hamiltonian coefficients can be smaller than the latter number, e.g., for the $(0, 1) \rightarrow (1, 1)$ vibrational $E2$ transition in HD^+ the numbers are 10 transitions (in f_t^{spin}) vs $9 + 9 = 18$ coefficients. The reason is the algebraic structure of the spin Hamiltonian.

We showed that by an extended combination ($f_t^{\text{pert-freee}}$) of Zeeman-resolved transition frequencies not only the spin structure, but also the four contributions: linear Zeeman, quadratic Zeeman, electric quadrupole, and tensor Stark shift can be canceled simultaneously. The scalar Stark shift, for which a cancellation cannot occur if only a single rovibrational transition is addressed, is at the 10^{-16} level for particular suitably chosen rovibrational transitions, for both H_2^+ and HD^+ .

We also showed that “economic” combinations of transition frequencies, f_t^{opt} , can also provide both spin-structure and external-field-shifts cancellations.

A more limited case is spin-structure-shift cancellation and nulling of the LZ shift ($f_t^{\text{spin,LZ}}$), which can be achieved simultaneously by specifically interrogating only the $J_z = 0 \rightarrow J'_z = 0$ components or the $J_z = -1/2 \rightarrow J'_z = -1/2$ and $J_z = 1/2 \rightarrow J'_z = 1/2$ component pairs in the case of systems with integer or half-integer angular momentum, respectively. The QZ, the EQ, and Stark shifts then remain present.

We have treated the particular systems H_2^+ , HD^+ in detail because of a specific metrological application of these molecules, but the treatment is applicable to any quantum system with spin structure. The potential utility of the proposed approach is clearly highest when applied to rotational transitions, where the contributions of the spin energies and of the systematic shifts to the transition frequency are, in fractional terms, approximately two orders larger than for vibrational frequencies. The metrological interest of rotational transitions of the molecular hydrogen ions is as follows. A rotational frequency is closely proportional to $R_\infty m_e/\mu$, where μ is the reduced nuclear mass. Vibrational transition frequencies between levels having small v, v' are instead closely proportional to $R_\infty \sqrt{m_e/\mu}$. Therefore, the measurement of one spin-averaged rotational frequency and one vibrational frequency and comparison with *ab initio* predictions can lead to an *independent* determination of R_∞ and m_e/μ .

For H_2^+ the implementation of the proposed method appears promising. If the rovibrational level $(v = 0, N = 0)$ or $(v = 0, N = 2)$ is chosen as the initial level, *just two* spin-resolved transitions need to be measured in order to cancel the spin structure of a vibrational transition. Moreover, these levels are very suitable for spectroscopy because they contain only a single or two spin states, respectively, so that their preparation is simplified [22]. Third, some of the Zeeman components exhibit very small systematic effects already individually [8,9]. Two particular combinations of four Zeeman components cancel both the LZ and the QZ shift, leaving as dominant shift the EQ shift of approximately 1×10^{-14} in the more advantageous of the two. If in addition the EQ shift is to be removed, five transitions are to be measured, leading to a residual (Stark) shift of 1×10^{-16} .

For HD^+ the implementation effort is, at first sight, larger, because of the more complex spin structure: for example, 10 Zeeman components need to be measured in order to extract the spin-averaged frequency of the fundamental rotational or vibrational transition. However, with proper choice of the Zeeman components, the LZ shifts are canceled with the same number of transitions. We have proposed to use an $E2$ transition, and again 10 Zeeman components, so as to reduce the other systematic shifts to the low- 10^{-13} level.

The shifts can be completely nulled by increasing to 14 or 16 the number of Zeeman components to be measured. Then, only the scalar Stark shift remains, of order 10^{-16} for the $E2$ transitions.

This level is comparable to that arising from blackbody radiation at 300 K, since the rms electric field assumed here is similar to that produced by the radiation at this temperature.

The above discussion has treated explicitly the cases of small rotational angular momenta $N = 0, 1, 2$, so it included the fundamental rotational transitions, $(v = 0, N = 0) \rightarrow (0, 1)$ for HD^+ and $(v = 0, N = 0) \rightarrow (0, 2)$ for H_2^+ , but is not limited to these.

Rotational transition frequencies can also be determined indirectly, via subtraction of vibrational transition frequencies. This can be an effective approach in the case of H_2^+ , for which a suitable source for driving the $E2$ fundamental rotational transition at 5.3 THz may not be available, but which can also be obtained as $f(0, 0 \rightarrow v', 2) - f(0, 2 \rightarrow v', 2)$. In order to achieve the spin-structure independence

of this computed rotational frequency, the present approach would be applied to the two contributing vibrational transitions (see Table VII).

The vibrational transitions discussed here were the fundamental ones, $v = 0 \rightarrow v' = 1$. The results will be similar for the overtones $v = 0 \rightarrow v' > 1$. The fractional residual shifts will decrease with increasing v' since the shifts themselves do not scale with v' .

Finally, we emphasize that the concept of traceless frequency is valuable and can be applied irrespective of future progress in the *ab initio* theory of the spin Hamiltonian. Of course such progress is important, allowing experimental

tests of the higher-order-in- α corrections to the spin Hamiltonian coefficients by probing *individual* spin components. Concerning experimental feasibility of the present proposal we remark that already in Ref. [3] a large number (11) of hyperfine components of a particular rovibrational transition were measured. Thus the experimental effort necessary to determine traceless frequencies appears manageable.

ACKNOWLEDGMENTS

V.I.K. acknowledges support from the Russian Science Foundation under Grant No. 18-12-00128.

-
- [1] V. I. Korobov, L. Hilico, and J.-P. Karr, Fundamental Transitions and Ionization Energies of the Hydrogen Molecular Ions with Few ppt Uncertainty, *Phys. Rev. Lett.* **118**, 233001 (2017).
 - [2] J. C. J. Koelemeij, B. Roth, A. Wicht, I. Ernsting, and S. Schiller, Vibrational Spectroscopy of HD⁺ with 2-ppb Accuracy, *Phys. Rev. Lett.* **98**, 173002 (2007).
 - [3] U. Bressel, A. Borodin, J. Shen, M. Hansen, I. Ernsting, and S. Schiller, Manipulation of Individual Hyperfine States in Cold Trapped Molecular Ions and Application to HD⁺ Frequency Metrology, *Phys. Rev. Lett.* **108**, 183003 (2012).
 - [4] J. Biesheuvel, J.-P. Karr, L. Hilico, K. S. E. Eikema, W. Ubachs, and J. C. J. Koelemeij, Probing QED and fundamental constants through laser spectroscopy of vibrational transitions in HD⁺, *Nat. Commun.* **7**, 10385 (2016).
 - [5] S. Alighanbari, M. Hansen, V. Korobov, and S. Schiller, Rotational spectroscopy of cold and trapped molecular ions in the Lamb-Dicke regime, *Nat. Phys.* **14**, 555 (2018).
 - [6] V. I. Korobov, J. C. J. Koelemeij, L. Hilico, and J.-P. Karr, Theoretical Hyperfine Structure of the Molecular Hydrogen Ion at the 1 ppm Level, *Phys. Rev. Lett.* **116**, 053003 (2016).
 - [7] K. Pachucki and V. A. Yerokhin, Theory of the helium isotope shift, *J. Phys. Chem. Ref. Data* **44**, 031206 (2015).
 - [8] J.-P. Karr, S. Patra, J. Koelemeij, J. Heinrich, N. Silltoe, A. Douillet, and L. Hilico, Hydrogen molecular ions: New schemes for metrology and fundamental physics tests, in *8th Symposium on Frequency Standards and Metrology 2015*, edited by F. Riehle [*J. Phys.: Conf. Ser.* **723**, 012048 (2016)].
 - [9] S. Schiller, D. Bakalov, and V. I. Korobov, Simplest Molecules as Candidates for Precise Optical Clocks, *Phys. Rev. Lett.* **113**, 023004 (2014).
 - [10] C. Schwarz, Theory of Hyperfine Structure, *Phys. Rev.* **97**, 380 (1955).
 - [11] D. Bakalov and S. Schiller, The electric quadrupole moment of molecular hydrogen ions and their potential for a molecular ion clock, *Appl. Phys. B* **114**, 213 (2014); **116**, 777 (2014).
 - [12] S. Schiller, D. Bakalov, A. K. Bekbaev, and V. I. Korobov, Static and dynamic polarizability and the Stark and blackbody-radiation frequency shifts of the molecular hydrogen ions H₂⁺, HD⁺, and D₂⁺, *Phys. Rev. A* **89**, 052521 (2014).
 - [13] D. Bakalov, V. Korobov, and S. Schiller, External-field shifts in precision spectroscopy of hydrogen molecular ions, *Hyperfine Interact.* **233**, 109 (2015).
 - [14] D. Bakalov, V. I. Korobov, and S. Schiller, High-Precision Calculation of the Hyperfine Structure of the HD⁺ Ion, *Phys. Rev. Lett.* **97**, 243001 (2006).
 - [15] V. I. Korobov, L. Hilico, and J.-P. Karr, Hyperfine structure in the hydrogen molecular ion, *Phys. Rev. A* **74**, 040502 (2006).
 - [16] D. Bakalov, V. I. Korobov, and S. Schiller, Magnetic field effects in the transitions of the HD⁺ molecular ion and precision spectroscopy, *J. Phys. B: At., Mol., Opt. Phys.* **44**, 025003 (2011); Corrigendum: Magnetic field effects in the transitions of the HD⁺ molecular ion and precision spectroscopy, **45**, 049501 (2012).
 - [17] For example, an analytical calculation of the diagonal matrix elements of the Breit-Pauli Hamiltonian can be performed in the basis of the states $(I_p, I_{p,z}), (I_d, I_{d,z}), (s_e, s_{e,z}),$ and (N, N_z) with $I_p = 1/2, I_d = 1,$ and $s_e = 1/2$. Taking the sum over these elements must yield zero. One can also verify tracelessness for many rovibrational levels computed in previous work, by performing the weighted average, Eq. (2), over the numerical values of the spin energies given in Table III of Ref. [14]. The sum rule for the QZ shifts can also easily be verified numerically as follows. By summing over all entries in the middle lines of Table 2 in Ref. [16] (the values q^{vLn}) one verifies the case $J_z = 0$. The cases $J_z \neq 0$ can be verified by appropriate sums over the middle and lower lines together, omitting those entries belonging to states having $J < |J_z|$.
 - [18] J. Shen, A. Borodin, M. Hansen, and S. Schiller, Observation of a rotational transition of trapped and sympathetically cooled molecular ions, *Phys. Rev. A* **85**, 032519 (2012).
 - [19] J.-P. Karr, F. Bielsa, A. Douillet, J. Pedregosa Gutierrez, V. I. Korobov, and L. Hilico, Vibrational spectroscopy of H₂⁺: Hyperfine structure of two-photon transitions, *Phys. Rev. A* **77**, 063410 (2008).
 - [20] V. I. Korobov, P. Danev, D. Bakalov, and S. Schiller, Laser-stimulated electric quadrupole transitions in the molecular hydrogen ion H₂⁺, *Phys. Rev. A* **97**, 032505 (2018).
 - [21] K. B. Jefferts, Hyperfine Structure in the Molecular Ion H₂⁺, *Phys. Rev. Lett.* **23**, 1476 (1969).
 - [22] S. Schiller, I. Kortunov, M. Hernández Vera, F. Gianturco, and H. da Silva, Quantum state preparation of homonuclear molecular ions enabled via a cold buffer gas: An ab initio study for the H₂⁺ and the D₂⁺ case, *Phys. Rev. A* **95**, 043411 (2017).